Journal of Thermal Analysis and Calorimetry, Vol. 67 (2002) 135–146

THERMAL BEHAVIOUR OF METAL COMPLEXES OF 6-(2-PYRIDYLAZO)-3-ACETAMIDOPHENOL

G. G. Mohamed, F. A. Nour El-Dien and Nadia E. A. El-Gamel*

Chemistry Department, Faculty of Science, Cairo University, Giza, Egypt

Abstract

The present work aims chiefly to study the thermal behaviour of complex compounds with general formula: $[M(HL)\cdot xH_2O](A)\cdot yH_2O$ (where HL=$C_{13}H_{11}N_4O_2$=6-(2-pyridylazo)-3-acetamidophenol (PAAP), M=Cu(II), Zn(II), Cd(II) and Fe(III) x=1, 3; y=2, 5) while A=CH_3COO^- (Ac), Cl_2. The second formula is $[M(H_2L)\cdot xH_2O]Cl_2\cdot yH_2O$, (where H_2L=$C_{13}H_{12}N_4O_2$ (PAAP), M=Ni(II), Co(II) x=3; y=4, 6). The compounds were identified by elemental analysis, FT-IR spectra and TG/DTG, DTA methods. It was found that during the thermal decomposition of complex compounds water molecules of crystallization are released in the first step. In the next step the pyrolysis of organic ligand takes place. Metal oxide remained as a solid product of the thermal decomposition. Mass spectroscopy has been used for the determination of the thermal decomposition on the intermediate products. It was found that the thermal stability of the studied compounds increases as the ionic radii decreases. The activation energy E, the entropy change ΔS^*, the enthalpy ΔH^* change and Gibbs free energy change ΔG^* were calculated from TG curve.

Keywords: cadmium(II), cobalt(II), copper(II), DTA, DTG, iron(III), mass spectrometry, nickel(II), TG, 6-(2-pyridylazo)-3-acetamidophenol complexes, thermal behaviour, transition metals, zinc(II)

Introduction

The importance of 6-(2-pyridylazo)-3-acetamidophenol and its metal chelates may stem from its biological activity and analytical investigation [1, 2]. Heterocyclic azodyes were widely applied as reagents for the determination of microamounts of transition elements [3, 4] and rare earth elements [5, 6]. For the last 30 years, various highly sensitive heterocyclic azo phenols were synthesized and examined as spectrophotometric reagents for microdetermination of various metal ions [7]. They were used to prepare different transition metal complexes [8–10]. The thermal analysis techniques were widely applied in studying of thermal behaviour of metal complexes [11–14]. The stoichiometry of thermal decomposition of some 2-substituted pyridines was studied by Jona *et al.* [15].

* Author to whom all correspondence should be addressed. E-mail: mazayed@chem-sci.cairo.eun.eg

1418–2874/2002/ $ 5.00

Akadémiai Kiadó, Budapest
Kluwer Academic Publishers, Dordrecht

Azo compounds containing cetamol nucleus have been paid little attention by analytical chemists. Literature scantly concerns the metal complexes of pyridylazo-acetamidophenol (PAAP). Therefore, the main target of this study is to determine the thermal behaviour of its metal complexes and how it is correlated with the fragmented ion peaks resulted from the mass spectra. Different activation thermodynamic parameters are calculated from TG curves.

Experimental

Synthesis of 6-(2-pyridylazo)-3-acetamidophenol (PAAP)

2-Aminopyridine 9.4 mg (0.1 mol) was mixed with 3.1 cm^3 HCl (10 M) and diazotized below 5°C with 6.9 mg $NaNO_2$ (0.1 mol). The resulting diazonium chloride was coupled with an alkaline solution of 15.1 mg 3-acetamidophenol (0.1 mol) below 0°C. The product was filtered off, crystallized from diethylether and dried over vacuum calcium chloride to get a final pure dye, yield 50% with red color. The melting point of the pure solid azo product was 82°C.

Synthesis of the metal complexes

The metal complexes were prepared by the addition of ammoniacal solution of the appropriate metal chloride or acetate (0.01 mol) in 25 mL ethanol-water mixture (1:1) to the solution of the 2.56 mg (0.01 mol) azo compound in 50 mL of the same solvent. The resulting mixture was stirred under reflux for half an hour at 60–70°C whereupon the complexes were precipitated. They were collected by filtration, washed with 1:1 ethanol:water mixture and finally with diethylether. The melting points of metal complexes were higher than 300°C.

Instruments

The elemental analyses for C, H and N of these complexes were performed by Heraeus instrument. Infrared spectra were recorded on a Perkin Elmer FT-IR type 1650 spectrophotometer. ^{1}H NMR spectrum was recorded on Varian Gemini 200 spectrometer (200 MHz ^{1}H NMR). The thermogravimetric analysis (TG/DTG) and differential thermal analysis DTA were carried out in dynamic nitrogen atmosphere (20 cm^3 min^{-1}) with a heating rate of 10°C min^{-1} using a Shimadzu TGA-50H and DTA-50H Thermal Analyzers. The activation energy E^* was calculated from TG curve by Coats-Redfern [16] method. The mass spectra were recorded with EI technique at 70 eV on a Hewlett-Packard Model MS-5988 GS-MS instrument.

Table 1 Analytical and physical data of 6-(2-pyridylazo)-3-acetamidophenol and its complexes

Compound	Colour (% yield)	*m. p.*/ °C	Found (calcd.)/%				Molecular mass found (calcd.)	μ_{eff} / B. M.	Conductance / Ω^{-1} cm^2 mol^{-1}
			C	H	N	M			
Ligand [H_2L]	red (70)	80	60.07 (60.9)	4.3 (4.6)	21.7 (21.87)		256 (256)	–	–
[$Fe(C_{13}H_{11}N_4O_2)(H_2O)_3$]$Cl_2$	black (70)	>300	37.05 (35.8)	5.1 (3.9)	13.2 (12.84)	13.3 (12.84)	440 (436)	4.29	455
[$Co(C_{13}H_{12}N_4O_2)(H_2O)_3$]$Cl_2 \cdot 4H_2O$	dark red (63)	>300	29.2 (30.4)	4.9 (5.8)	10.78 (10.9)	11.34 (11.53)	511 (512)	5.0	238
[$Ni(C_{13}H_{12}N_4O_2)(H_2O)_3$]$Cl_2 \cdot 6H_2O$	rose (60)	>300	27.9 (28.5)	5.9 (6.0)	10.13 (10.23)	10.3 (10.8)	551 (548)	3.82	161
[$Cu(C_{13}H_{11}N_4O_2)(H_2O)$](Oac)$\cdot 5H_2O$	dark red (73)	>300	34.6 (32.13)	5.2 (4.73)	11.15 (11.53)	12.7 (13.08)	495 (485.5)	1.89	117
[$Zn(C_{13}H_{11}N_4O_2)(H_2O)$](OAc)$\cdot 2H_2O$	dark red (73)	>300	40.4 (41.4)	5.0 (4.8)	12.89 (12.93)	14.95 (15.01)	437 (433)	Diam.	125
[$Cd(C_{13}H_{11}N_4O_2)(H_2O)$]Cl$\cdot 5H_2O$	brown (73)	>300	29.5 (30.5)	3.8 (4.6)	10.9 (10.96)	21.76 (21.93)	511 (510.5)	Diam.	67

Results and discussion

Properties, FT- IR and NMR characteristics of the synthesized compounds

The prepared complex compounds are stable when kept on light in air at room temperature. The experimental and calculated C, H, N values are in good agreement with the proposed structures (Table 1).

IR spectra reveal the presence of ν(OH) band of the phenolic group at 3566 cm^{-1}. The ν(NH) and ν(C=O) bands of acetamide group appear at 3398 and 1699 cm^{-1}, respectively. The ν(C–N) band of the pyridine ring appears at 1321 cm^{-1} and that of ν(N=N) band of the azo group at 1522 cm^{-1}.

The present ligand is also confirmed by ^{1}H NMR spectra in DMSO. Methyl group of acetamide gives signals at δ=2.53 ppm (strong, 3H). The δ=6.18–8.07 ppm refers to (medium, 6H) aryl and pyridine protons, respectively. The δ=10.45 (broad, 1H) is due to proton of NH group and that of δ=14.0 ppm (strong, 1H) is due to proton of OH group of phenyl ring. As usual signals due to NH and OH groups protons are hidden in deuterated solvent.

The thermal behaviour of the prepared compounds

In the following paragraphs the thermal behaviour of the synthesized compounds, characterized on the basis of TG/ DTG, DTA, and mass spectroscopy are described.

$[Fe\ (C_{13}H_{11}N_4O_2)\ (H_2O)_3]Cl_2$

The compound slowly started to decompose at 60°C (Fig. 1a). The first mass loss (8.71% est.; 8.37% calc.) up to 220°C is in a good agreement with the loss of one molecule HCl. The DTA curve shows an exothermic peak at 250°C. This is immediately followed by exothermic process at 350°C with mass loss (70.12% est.; 72.82% calc.) between 220–650°C, due to the pyrolysis of organic molecule and HCl. The remainder ferric hydroxide [17], was detected also by the mass spectra (*m*/*z* = 108) and it undergoes further decomposition to ferric oxide.

$$[Fe(C_{13}H_{11}N_4O_2)(H_2O)_3]Cl_2 \xrightarrow[60-220^{o}C]{-HCl} [Fe(C_{13}H_{11}N_4O_2)(OH)(H_2O)_2]Cl$$

$$[Fe(C_{13}H_{11}N_4O_2)(OH)(H_2O)_2]Cl \xrightarrow[220-650^{o}C]{-C_{13}H_{15}N_4O_2,\ -HCl} Fe(OH)_3 \longrightarrow Fe_2O_3 + 3H_2O$$

$[Co\ (C_{13}H_{12}N_4O_2L)\ (H_2O)_3]Cl_2$

The cobalt complex decomposed in several overlapped decomposition steps (Fig. 1b). The mass loss (27.70% est.; 28.30% calc.) is attributed to the removal of four hydrated water, three coordinated water and CH_4 molecules. This process is accompanied by two exothermic process at 290 and 360°C in DTA curve. The activa-

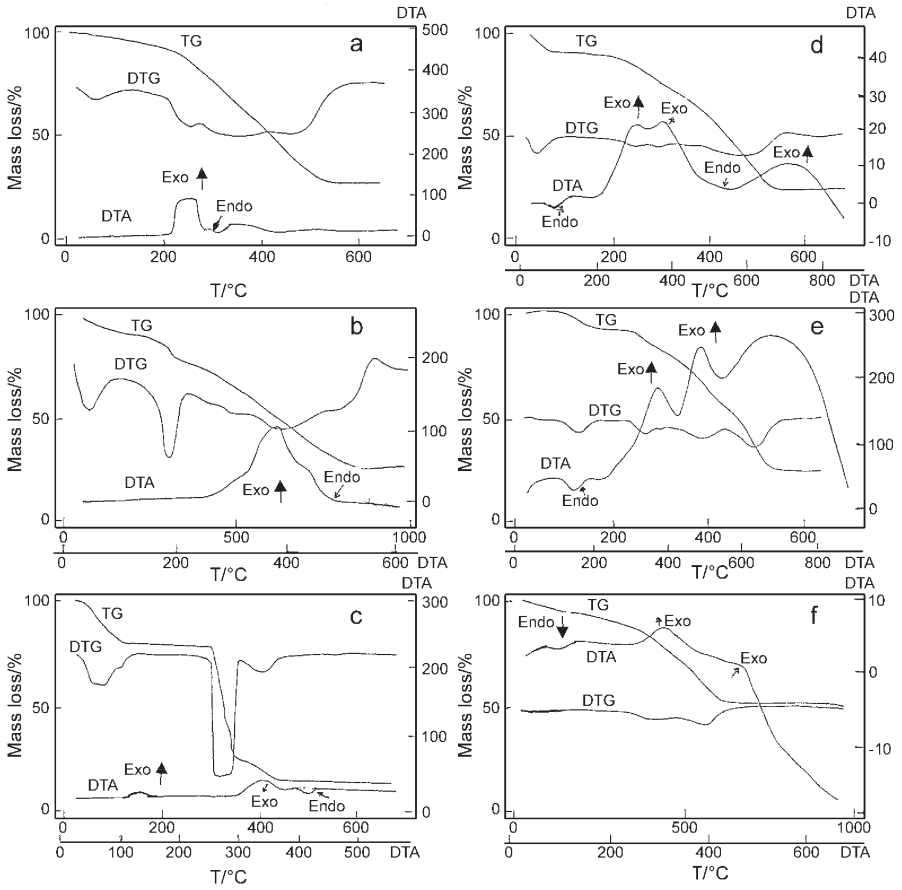

Fig. 1 Thermal analyses (TG and DTA) of 6-(2-pyridylazo)-3-acetamidophenol:
a – Fe(III), b – Co(II), c – Ni(II), d – Cu(II), e – Zn(II) and f – Cd(II) complexes

tion energy for this step is found to be 27.83 kJ mol^{-1}. In the temperature range 415 till 995°C the mass loss (46.09% est.; 46.31% calc.) is accompanied in the TG curve by two endothermic processes at 430 and 454°C. This decomposition is due to the pyrolysis of the ligand molecule. The final products of the thermal decomposition $CoCl_2$ (m/z=131) [17] were determined by means of mass spectra.

$$[Co(C_{13}H_{12}N_4O_2)(H_2O)_3]Cl_2 \cdot 4H_2O \xrightarrow[60-415^{o}C]{4H_2O + 3H_2O + CH_4} [Co(C_{13}H_{12}N_4O_2)]Cl_2$$

$$[Co(C_{13}H_{12}N_4O_2)]Cl_2 \xrightarrow{415-995^{o}C} CoCl_2 + C_{12}H_8N_4O_2$$

$[Ni\ (C_{13}H_{12}N_4O_2)\ (H_2O)_3](Cl)_2{\cdot}6H_2O$

The thermal decomposition of this complex starts (Fig. 1c) at 50°C. The first mass loss was (20.40% est.; 19.89% calc.) due to the loss of two hydrated water and two HCl gas molecules in the temperature range 50–225°C. It was accompanied by an exothermic process at 120°C in DTA curve. The formula of the intermediate solid product $[Ni\ (C_{13}H_{12}N_4O_2)\ (H_2O)_3](OH)_2{\cdot}2H_2O]$ of the thermal decomposition was proved by elemental analysis and FT-IR spectra. The next step of the thermal decomposition is followed by an exothermic process at 315°C in DTA curve. It is due to the complete decomposition of organic ligand (50.30% est.; 50.0% calc.). The remaining nickel oxide was detected by mass spectra (*m*/*z*=75).

$$[Ni\ (C_{13}H_{12}N_4O_2)(H_2O)_3]Cl_2{\cdot}6H_2O \xrightarrow[50-225\,^{o}C]{2HCl+2H_2O} [Ni\ (C_{13}H_{12}N_4O_2)\ (H_2O)_3](OH)_2{\cdot}2H_2O$$

$$[Ni\ (C_{13}H_{12}N_4O_2)\ (H_2O)_3](OH)_2{\cdot}2H_2O \xrightarrow{250-360\,^{o}C} C_{13}H_{12}N_4O_2 + H_2O$$

$$[Ni(H_2O)_4(OH)_2] \xrightarrow[360-550\,^{o}C]{5H_2O} NiO$$

$[Cu\ (C_{13}H_{11}N_4O_2)\ (H_2O)]Ac{\cdot}5H_2O$

On the other hand, acetate complex exhibits the first mass loss of (11.40% est.; 11.10% calc.) in the temperature range 50–160°C with an endothermic process on the DTA curve at 87°C (Fig. 1d). It may be attributed to the liberation of three molecules of hydrated water. The activation energy of this dehydration step is 71.45 kJ mol^{-1}. The second mass loss at 160–265°C (7.40% est.; 7.40% calc.) with an exothermic process at 263°C is due to the liberation of last two water molecules. The formation of solid complex $[Cu(C_{13}H_{11}N_4O_2)\ (H_2O)]Ac$ (*m*/*z*=395) was detected by the mass spectra. The solid intermediate complex starts to decompose (65.90% est.; 65.20% calc.) in the temperature range 270–620°C by an exothermic and an endothermic process at 351 and 418°C, respectively, in DTA curve. This is accompanied by the pyrolysis of the organic ligand and the evolution of CH_4 and the water molecule. Copper carbonate [17] was found as the solid product of the thermal decomposition.

$$[Cu\ (C_{13}H_{11}N_4O_2)\ (H_2O)]Ac{\cdot}5H_2O \xrightarrow[50-160\,^{o}C]{-3H_2O} [Cu\ (C_{13}H_{11}N_4O_2)\ (H_2O)]Ac\cdot 2H_2O$$

$$[Cu\ (C_{13}H_{11}N_4O_2)\ (H_2O)]Ac\cdot 2H_2O \xrightarrow{160-265\,^{o}C} -2H_2O + [Cu\ (C_{13}H_{11}N_4O_2)\ (H_2O)]Ac$$

$$[Cu\ (C_{13}H_{11}N_4O_2)\ (H_2O)]Ac \xrightarrow{270-620\,^{o}C} -H_2O - CH_4 - C_{13}H_{10}N_4O + CuCO_3$$

$[Zn\ (C_{13}H_{11}N_4O_2)(H_2O)]Ac{\cdot}2H_2O$

The TG curve of the Zn(II) complex indicates (Fig. 1e) that the complex decomposed in four steps. The first one in the temperature range of 60–200°C (8.80% est.; 8.30% calc.) with an endothermic effect on the DTA at 130°C which is due to the loss of two molecules of hydrated water. The activation energy of this dehydration step is 106.1 kJ mol^{-1}. The loss of coordinated water and CO_2 occurs at the temperature range 200–320°C. The last estimated mass loss in the temperature range 325–555°C attributed to the decomposition of organic ligand. This temperature is higher than in the case of other complexes, which may be due to the stronger bond between the zinc and ligand molecule. The solid product zinc oxide was detected by mass spectra (*m*/*z*=80).

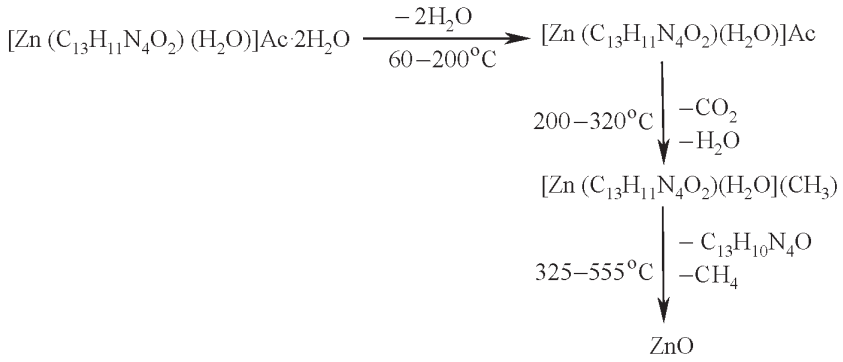

$[Cd\ (C_{13}H_{11}N_4O_2)(H_2O)]Cl{\cdot}5H_2O$

This complex starts to decompose (Fig. 1f) in the temperature range of 50–270°C. The first mass loss (6.97% est.; 7.05% calc.) with an endothermic process at 70°C in DTA curve, is due to the loss of two water molecules of hydration. This is followed immediately by the second mass loss (17.73% est.; 17.73% calc.) and third mass loss (25.66% est.; 25.85% calc.) within the temperature range 270–775°C with exothermic processes at 276 and 460°C in DTA curve. It corresponds to the liberation of HCl and pyrolysis of the organic ligand. The final residue of the thermal decomposition $Cd(NO_3)_2$ (*m*/*z*=237) [17] was proved by means of mass spectra.

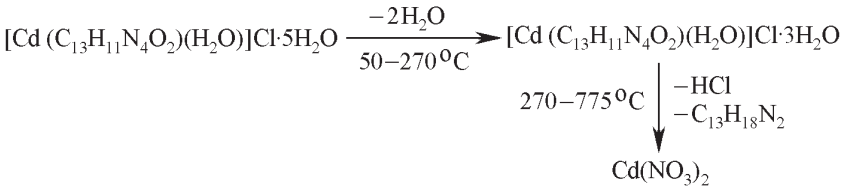

Table 2 Thermoanalytical results (TG, DTG, DTA) of the di- and trivalent d-block metal complexes of PAAP

Complex	TG range/ °C	DTG_{max}/°C	Peak temp. in DTA/°C	Mass loss estim. (calc%)*	Assignment
$[Fe(C_{13}H_{11}N_4O_2)(H_2O)_3]Cl_2$	60–220	60	250(–)	8.70 (8.4)	Loss of one HCl gas
	220–650	400	350(–)	67.10 (67.1)	Loss of ligand molecule and HCl gas
				75.80* (75.50)	leaving Fe_2O_3 residue
$[Co(C_{13}H_{12}N_4O_2)(H_2O)_3]Cl_2{\cdot}4H_2O$	60–415	66,300	290,360(–)	27.70 (28.30)	Loss of $4H_2O$, $3H_2O$ (coord.), and CH_4 molecules
	415–995	437,646,900	430,454(+)	46.09 (46.31)	Loss of ligand molecule leaving $COCl_2$
				73.79* (74.61)	residue
$[Ni(C_{13}H_{12}N_4O_2)(H_2O)_3]Cl_2{\cdot}6H_2O$	50–225	77	53,120(–)	20.40 (19.89)	Loss of $2H_2O$ molecules and 2HCl gas
	250–360	327	315(–)	50.30 (50.0)	Loss of one H_2O and ligand molecules
	360–550	400	390(–),420(+)	17.20 (17.30)	Loss of $5H_2O$ molecules leaving NiO
				87.90* (87.20)	residue
$[Cu(C_{13}H_{11}N_4O_2)(H_2O)](OAc){\cdot}5H_2O$	50–160	44	87(+)	11.40 (11.10)	Loss of $3H_2O$ molecules
	160–265	245	263(–)	7.40 (7.40)	Loss of $2H_2O$ molecules
	270–550	472	351(–),418(+)	56.90 (56.20)	Loss of H_2O (coord.) and ligand molecules leaving $CuCO_3$ residue
			,		
			642(–)	75.70* (74.70)	Phase transition
			823(+)		
$[Zn(C_{13}H_{11}N_4O_2)(H_2O)](OAc){\cdot}2H_2O$	60–200	127	130(+)	8.80 (8.30)	Loss of $2H_2O$ molecules
	200–320	272	–	13.20 (14.32)	Loss of H_2O and CO_2
	325–445	387	370(–)	24.90 (25.17)	Loss of $½N_2$, CH_4 and C_5H_5N molecules
	445–555	497	450(–)	34.20 (33.49)	Loss of $½N_2$, and C_8H_5NO molecules leaving ZnO residue
			700(–)	81.10* (81.28)	Phase transition
$[Cd(C_{13}H_{11}N_4O_2)(H_2O)]Cl{\cdot}5H_2O$	50–270	73	70(+)	6.97 (7.05)	Loss of $2H_2O$ molecules
	270–460	296,414	276(–)	17.73 (17.73)	Loss of HCl gas and ligand molecules
	460–775	567	460(–)	25.66 (25.85)	leaving $Cd(NO_3)_2$ residue
				49.90* (49.80)	

(+): endothermic, (–): exothermic
* Total mass loss

Calculation of activation thermodynamic parameters of the decomposed complexes

The thermodynamic activation parameters of the decomposition process of dehydrated complexes such as activation energy (E^*), enthalpy (ΔH^*), entropy (ΔS^*) and free energy of the decomposition (ΔG^*), were evaluated graphically by employing the Coats–Redfern [16] method using the relation:

$$\log\left[\frac{\log\{W_f/(W_f-W)\}}{T^2}\right]=\log\left[\frac{AR}{\theta E^*}\left(1-\frac{2RT}{E^*}\right)\right]-\frac{E^*}{2.303RT} \quad (1)$$

where W_f is the mass loss at the completion of the reaction, W is the mass loss up to temperature T, R is the gas constant, E is the activation energy in kJ mol^{-1} and θ is the heating rate.

Since $1-2RT/E^* \cong 1$, a plot of the left-hand side of Eq. (1) *vs.* $1/T$ gives a slope from which E^* was calculated and A (Arrhenius constant) was determined from the intercept (Table 3).

The calculated values of E^*, A, ΔS^*, ΔH^* and ΔG^* for the decomposition steps are given in Table 3. According to the kinetic data obtained from DTG curves, all the complexes have a negative entropy, which indicates that the studied complexes have more ordered systems than reactants.

The activation energy E^* and Gibbs free energy ΔG^* (Fig. 2) change with the increase of atomic number in the 3rd series of d-block elements, for the first decomposition step of their complexes with PAAP. The complexes of Fe^{3+} (d^5), Ni^{2+} (d^8) and Zn^{2+} (d^{10}) with PAAP are present on the top peaks of the energy curve. This means that these complexes are more stable at the beginning of the decomposition than those on the bottom of the curve Co^{2+} (d^7), Cu^{2+} (d^9) and Cd^{2+} (d^9) complexes. The same trend is gained for these complexes at the second steps of decomposition, except they

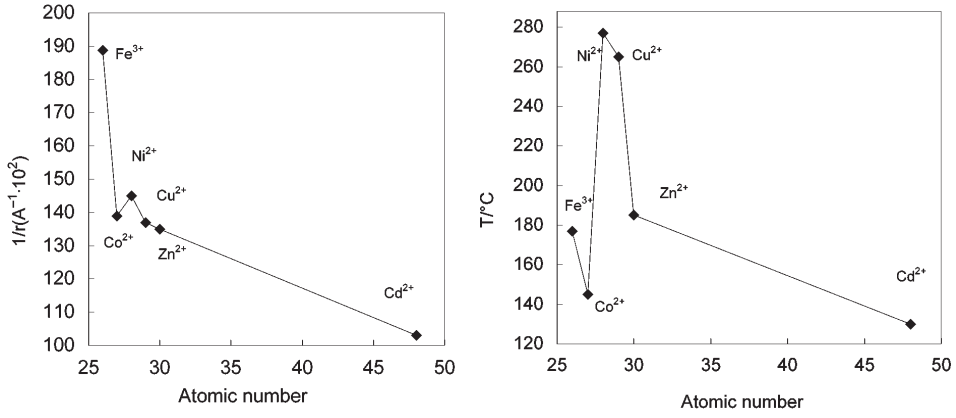

Fig. 2 Activation energy E^* and free energy change ΔG^* of di- and trivalent metal ions complexes of PAAP *vs.* atomic number: 1 – the first decomposition step, 2 – the second decomposition step

Table 3 Thermodynamic data of the thermal decomposition of di- and trivalent d-block metal ions-PAAP complexes

Complex	Decomposition range/°C	E^*/ kJ mol^{-1}	A/ s^{-1}	ΔS^*/ J K^{-1} mol^{-1}	ΔH^*/ kJ mol^{-1}	ΔG^*/ kJ mol^{-1}
$[Fe(C_{13}H_{11}N_4O_2)(H_2O)_3]Cl_2$	60–220	43.56	$1.60\cdot10^{6}$	–15.26	40.85	45.82
	220–650	160.2	$7.39\cdot10^{15}$	6.32	155.0	151.0
$[Co(C_{13}H_{12}N_4O_2)(H_2O)_3]Cl_2\cdot4H_2O$	60–415	27.83	$2.23\cdot10^{3}$	–21.88	25.04	32.40
	415–413	88.48	$2.13\cdot10^{7}$	–13.25	83.70	91.32
	413–995	40.38	9.18	–28.39	32.66	59.01
$[Ni(C_{13}H_{12}N_4O_2)(H_2O)_3]Cl_2\cdot6H_2O$	50–225	141.0	$8.30\cdot10^{22}$	23.24	138.3	130.8
	250–360	147.0	$2.28\cdot10^{21}$	19.58	144.1	137.5
	360–550	28.27	$5.22\cdot10^{2}$	–23.57	24.70	34.83
$[Cu(C_{13}H_{11}N_4O_2)(H_2O)](OAc)\cdot5H_2O$	50–160	71.45	$2.77\cdot10^{11}$	–3.18	68.82	69.82
	160–265	156.4	$3.67\cdot10^{15}$	5.827	152.1	149.1
	270–550	80.86	$8.10\cdot10^{4}$	–18.96	75.38	87.88
$[Zn(C_{13}H_{11}N_4O_2)(H_2O)](OAc)\cdot2H_2O$	60–200	106.1	$3.0\cdot10^{13}$	1.27	102.8	102.3
	205–325	227.2	$5.77\cdot10^{21}$	20.07	222.7	212.0
	320–445	127.7	$3.01\cdot10^{9}$	–8.43	122.2	127.8
	445–555	190.0	$2.19\cdot10^{12}$	–2.00	183.6	185.2
$[Cd(C_{13}H_{11}N_4O_2)(H_2O)]Cl\cdot5H_2O$	50–270	35.72	$3.38\cdot10^{4}$	–19.17	32.88	39.43
	270–460	89.78	$4.09\cdot10^{7}$	–12.57	85.13	92.16
	460–775	158.5	$8.17\cdot10^{11}$	–2.95	152.3	154.5

become excited before decomposition. The thermal behaviour of these complexes may be related to the decomposition of the ligand molecule of PAAP during thermal excitation. These quantitative explanations of results mean also that the thermal stability is mainly related to the stereo-structure of the complexes and the electronic configuration of the d-block elements. Therefore, pairing up energy P and energy of splitting of metal orbitals in octahedral Δ_0, tetrahedral Δ_t and square planner Δ_{sq} in strong environment are calculated. It is obvious that, those elements of Fe^{3+} (d^5) ($t_2g^5eg^0$, $\Delta_0 = -10/12-P$), Ni^{2+}(d^8) (t_2g^6 eg^2, $\Delta_0 = -6/12-2P$) and Zn^{2+} (d^{10}) (t_2g^6 eg^4, Δ_t=zero) are stable since they have high pairing up energy and even an electron system. The other elements of the odd electron system of Co^{2+} (d^7) (t_2g^6 eg^1, $\Delta_0 = -9/12$), Cu^{2+} (d^9) (t_2g^6 eg^3, $\Delta_{sq} = -3/12$) and Cd^{2+} (d^9) (t_2g^6 eg^3, $\Delta_t = -3/12$) have less stability due to the lower pairing effect. Fe^{3+} is present in the middle due to the competition between splitting and pairing up effect and its odd electron system. Zn^{2+} complex is present at the top of the curve, this may be due to the fact that Fe^{3+} has a half filled d-orbital while Zn^{2+} has a completely filled d-orbital. It can be concluded that, the relation between E^* and ΔG^* *vs.* atomic number gives a quantitative interpretation to the thermal stability of the complexes while the relation between the decomposition temperature and $(1/r)$ *vs.* atomic number gives a qualitative assignment.

In order to check the thermal stability of the complexes in the solid state, initial temperatures of the decomposition of the anhydrous complexes were compared. A plot of the initial decomposition temperatures of the anhydrous complexes and the corresponding reciprocal ionic radii of the tri- and divalent metal ions against the atomic number is shown in Fig. 3. The reciprocal of the ionic radii of the divalent metal ions decreases from Fe(III) to Co(II) with the decrease of initial temperatures of decomposition. While the reciprocal of the ionic radii increases from Co(II) to Ni(II) and the thermal stabilities of these complexes also increases. The same trend appears in comparing the thermal stabilities and the reciprocal of ionic radii from Ni(II) to Cd(II), which is found to decrease from Ni(II) to Cd(II). It is evident that the

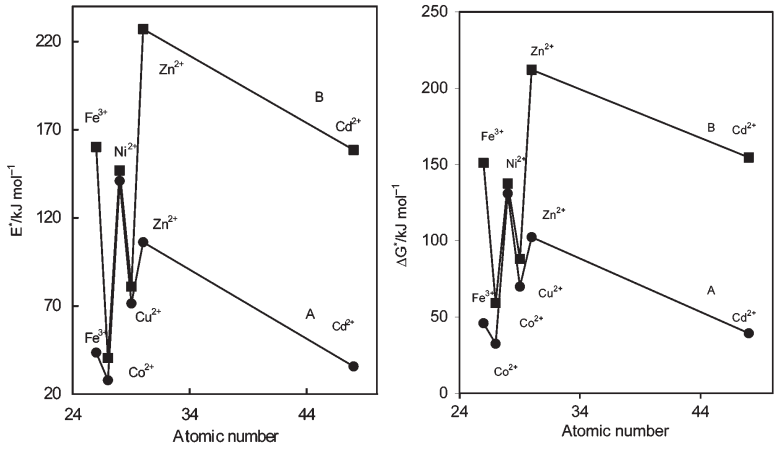

Fig. 3 Initial temperature of thermal decomposition of anhydrous complexes and reciprocals of ionic radii of di- and trivalent metal ions *vs.* atomic number

thermal stabilities of the complexes increase as the ionic radii decreased [18]. From the above results, it is qualitatively concluded that the thermal stability of the complexes follows the order

$$Ni(II) > Cu(II) > Zn(II) > Fe(III) > Co(II) > Cd(II).$$

The corresponding reciprocal ionic radii of the tri- and divalent metal ions against the atomic number exhibit the same definite trends.

* * *

We would like to present our deep thanks and gratitude to Prof. Dr. M. A. Zayed, for his effort and help in working this work in its present form.

References

1 A. Abu-Zuhri, Microchem. J., 29 (1984) 345.
2 Y. Wang, R. Yang, H. Yang, X. Wang and G. Zhang, Shaanxi Shifan Daxue Xuebao, Ziran Kexueban, 24 (1996) 68.
3 S. Balzamo, V. Carunchio, R. Galvani and A. Messina, Inorg. Chim. Acta, 97 (1985) 13.
4 I. V. Pyatnistskii, S. G. Mamuliya, K. I. Grigalashvili and L. L. Kolomiets, Ukr. Khim. Zh., 50 (1984) 977.
5 M. J. Sanchez, B. Santana, M. L. Perez Pont, V. Gonzalez and F. Garcia Montelongo, Polyhedron, 7 (1988) 495.
6 D. G. Gambarov, R. Z. Rzaev, F. N. Musaev, A. N. Musaeva and F. M. Chyragov, Zh. Neorg. Khim., 30 (1985) 72.
7 R. M. Awadallah, Asian J. Chem., 4 (1992) 511.
8 A. R. Casal, M. T. Goitia and M. E. Montero, Bol. Soc. Quim. Peru., 59 (1993) 1.
9 M. S. Sastry, R. Ghose and A. K. Ghose, Bull. Chem. Soc. (Ethiop.), 4 (1990) 61.
10 E. P. Potapova, M. I. Bulatov and V. V. Bardin, Izv. Vyssh. Uchebn. Zaved., Khim. Teckhnol., 35 (1992) 118.
11 M. A. Zayed and F. A. Nour El-Dien, Thermochim. Acta, 114 (1987) 359.
12 M. A. Zayed, M. M. Khater, M. S. Rizk and H. M. Abd El-Fattah, Thermochim. Acta, 73 (1984) 217.
13 A. A. Soliman, J. Therm. Anal. Cal., 63 (2001) 221.
14 A. F. Petrovic, D. M. Petrovic, V. M. Leovac and M. Budimir, J. Therm. Anal. Cal., 58 (1999) 589.
15 E. Jóna and M. Jamnicky, J. Thermal Anal., 27 (1987) 359.
16 A. W. Coats and J. P. Redfern, Nature, 201 (1964) 68.
17 D. R. Lide, CRC Hand Book of Chemistry and Physics 73rd Ed. 4, 1992–1993, pp. 46–112.
18 H. Icbudak, V. T. Yilmaz and H. Ölmez, J. Therm. Anal. Cal., 53 (1998) 843.